

Human-Adaptive Control of Series Elastic Actuators

Andrea Calanca, Paolo Fiorini

Abstract—Force controlled series elastic actuators (SEAs) are wide used components of novel physical human-robot interaction (pHRI) applications such as assistive and rehabilitation robotics. These systems are characterized by the presence of the “human in the loop” so that control response and stability depend on uncertain human dynamics. A common approach to guarantee stability is to use a passivity-based (PB) controller. Unfortunately existing PB controllers for SEAs do not define the performance of the torque/force loop. We propose a method to obtain predictable force/torque dynamics basing on adaptive control and oversimplified human models. We propose a class of stable human-adaptive algorithms and we experimentally show advantages of the proposed approach.

I. INTRODUCTION

Most of modern rehabilitation robotic systems make use of force controlled joints following the “assist as needed” paradigm. In this approach the patient is delicately guided to a target trajectory progressively reducing the interaction forces as the patient learns to better follow a desired path. In fact it has been shown that patients should be active to enable the motor learning process [12], [9], [3], thus rehabilitative devices should not be coercive. Several control algorithms have been proposed following this “assist as needed” approach e.g. “path control” [7], “virtual model control” [18], “clime” [25], gravity compensation [13], [6] or impedance control [25]. This class of algorithms is build upon a force/torque controller that is supposed to be ideally fast. However when the algorithm is implemented the force variable cannot be commanded instantaneously and its transients depend both on robot and patient dynamics. In particular, using a traditional controller we can have slow force/torque responses when the patient displays a low mechanical impedance and force/torque overshoots when the patient has a high impedance configuration. These effects are undesirable because they can generate disturbances that interfere with the rehabilitation strategy and even potentially lead to instability and patient injuries.

Currently a wide used method to guarantee stable human robot interaction is based on PB control. Despite complexity of passivity formalism, PB control is quite straight forward to implement [24], [26] and the whole stability can be guaranteed by assuming that humans behave in a passive way. Unfortunately in PB control it is not possible to give any servo specification, because the controller needs to be stable against any kind of external passive environment. No matter what kind of environment and no matter its scale, i.e. its level of inertia, stiffness or damping. It follows that this approach is very conservative and by completely neglect environmental dynamics it is not possible to speculate on control performance. To be said that this limit is not due to passivity itself but to the absence of a human model. As a matter of facts authors that propose passive controllers for rehabilitation or pHRI

usually do not comment about control tuning (that involves specifications). The implicit idea is of tuning the system trial and error, considering an average human dynamics and trying to match a desired transient. Then it is necessary to check if passivity constraints are satisfied [24]. However this strategy leads to the following considerations:

- 1) In our experience [5] it is quite difficult to carry out a tuning process with the human in the loop, both from the point of view of safety and of practical feasibility. Of course it is possible to couple the system to an artificial limb or a manikin but in these cases the solution will be quite approximate.
- 2) The tuning session can be time consuming. In fact if the passivity conditions are not satisfied in a first trial, it is necessary to reiterate the tuning until passivity is finally archived. In fact there is no method to verify passivity during the tuning process, unless a very simple control structure is assumed.
- 3) Pathologies can specifically affect limbs. With currently available PB controllers the tuning procedure should be carried out separately for each patient and for each patient joint. It follows that an automatic tuning process can be of paramount importance.
- 4) Humans typically change their dynamics in response to the environment and depending on the specific tasks. For example leg dynamics dramatically changes between the swing and the stance phase. Also damping and stiffness can be increased by muscle co-contraction like when we want to make a precise positioning or when we hold heavy loads.

To solve these issues we propose a model-based controller that automatically varies force control gains in response to changing conditions, to match the desired force/torque transient. Since the whole human modeling is unaffordable, it is reasonable to think that a simplified model can tell us at least something about the patient. In particular we approximate human joints and endpoints with second order linear models. Combining such generic models with adaptivity we meet two advantages: first using a generic model we can account for a generic human joint and second using adaptivity we can update model parameters as the situation changes, e.g. when a grasped mass is added or when co-contraction is modified. We propose an approach inspired by model reference adaptive control (MRAC) where control specifications can be determined by the reference model, letting the tuning process to be automatic and online adapting to changing conditions.

The paper is organized as follows. Section II presents the currently available solutions for SEA control in pHRI. Section III describes the system to be controlled and section IV introduces the proposed adaptive controller and gives a theoretical

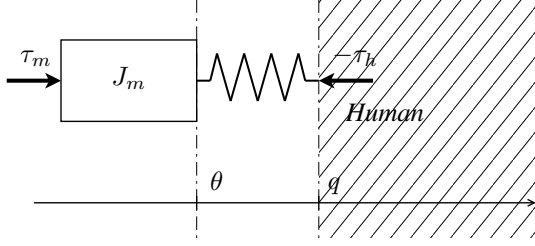


Figure 1. The model for series elastic actuator proposed in [16]. It includes the motor inertia, the elasticity and the coupling with the environment.

stability analysis. Experimental results are presented in section V. Finally conclusions are drawn in section VI together with future work plan.

II. SERIES ELASTIC ACTUATORS AND THEIR CONTROL

A. Series Elastic Actuators and Force Control

SEAs have been proposed to overcome force control difficulties that arise using stiff actuators [16]. In SEAs a spring is arranged between the motor and the environment, which in our case is a generic human joint. This is shown in figure 1 where τ_m is the motor force/torque, k is the series spring stiffness, θ is the motor position, τ_h is the human interaction force/torque and q is the human joint position. The relation among these variables can be expressed as

$$\tau_h = k(\theta - q) \quad (1)$$

$$J_m \ddot{\theta} = \tau_m - \tau_h \quad (2)$$

where the first equation describes the force exerted by the spring to the human and the second accounts for motor inertia J_m .

The main advantages of SEAs are the increased force control robustness, augmented shock tolerance and safety due to lower reflected inertia. Moreover force can be measured through spring deformation that is cheaper than using a load cell (in the case of force) or a rotative torsionmeter (in the case of torque).

To the authors knowledge all the proposed SEA implementations make use of high transmission ratios. For example: in [17] a screw ball with a pitch of 2mm per revolution (linear actuator) is used, whereas in [11] the transmission ratio is $n = 130$ (rotative actuator). The reason why SEAs usually employ reducers or gearboxes is to obtain high force and high power density. However a geared motor results very stiff and difficult to control in force. By adding a series spring, SEAs transform the force control problem into a position control problem (spring displacement) where high ratio transmissions are known to be helpful: the motor results stiffened and the effects of external disturbances are reduced.

B. Series Elastic Actuators and Robust Interaction Control

Currently the main technique used to stabilize pHRI is based on passivity theory. PB controllers are quite easy to implement and impressively robust as they are stable against any passive coupling. However nothing can assure us that a PB

controller is a “good controller”. For example, the passivity-based force controller proposed in [16] consists of a standard PID controller with an integral roll-off, as represented by

$$F(s) = P + \frac{Ds}{1 + T_d s} + \frac{I}{1/T_i + s} \quad (3)$$

where P , D and I are positive gains and the integral roll off must satisfy $T_i \leq \sqrt{D/I}$. The performance of this passive PID controller depends both on gain values and coupled environment whose dynamics is usually unknown and produces unknown control performance. For passivity analysis of different control architectures, including inner velocity loops and pure integrators, the reader can refer to [24] where it is shown that, depending on the architecture, the passivity constraint imposes upper or lower bounds on certain control gains. About passivity it is also reported by Hogan [1] that “discrete control, time delays, actuator and sensor limitations, and unmodeled dynamics can also compromise passivity, making the implementation of passive control on real systems extraordinarily challenging.”

A significantly different approach to pHRI control is described in [23] and is based on classic robust control and is not based on elastic actuators. This method potentially allows to account for specifications but it needs an accurate human model which is very hard to develop in practice. Another robust strategy have been applied to the case of a stiff motor and is reported in [2], [1]. Here the authors consider oversimplified models (linear second order) for the human and propose an automated procedure to search for a robust controller which is optimal in terms of both performances and stability. This is because classic robust methods provide only analysis tools to check the stability at the end of a design phase and in case of failure it is necessary to iterate between design and analysis phases. Also the robust design is a sub-optimal solution because the assumed model set needs to be conservative to include the uncertainty.

III. SYSTEM ANALYSIS

In this work we follow the approach of using second order linear models to approximate the human joint impedance¹. Such simple and general models have two main advantages. First they need fewer parameters to be adapted to. Second a single adaptive controller structure can work for every human joint and also for human endpoints, broadening the applicability of the approach.

In a first step we model the system by considering the human joint as a pure inertia J_h . In this case we have the following human model

$$J_h \ddot{q} = k(\theta - q) = \tau_h \quad (4)$$

to be considered together with SEA model (1) and (2). To describe the torque control application the overall model should be arranged with an input torque τ and an output torque τ_h . To this aim it is possible to arrange (1), (2) and (4) as

$$\frac{J_m}{k} \ddot{\tau}_h + (1 + \frac{J_m}{J_h}) \tau_h = \tau. \quad (5)$$

¹Although this oversimplification is quite rough, it is widely used (and tested) in literature, see for example [20], [10], [21], [27], [22], [15].

Note that this torque to torque relation results in a second order system in spite of being originally a fourth order system. The reason is because, if we do not account for friction and/or human joint stiffness, we have pole-zero cancellations. Thus the second order approximation is reasonable only in the case of a pure inertial load, otherwise a higher order system should be considered. In particular, the model becomes a third order in the presence of human joint damping and a forth order if we account also for stiffness, leading to the following equations

$$\frac{J}{k}\ddot{\tau}_h + (1 + \frac{J_m}{J_h})\tau_h - rh(q - q_0) - rd\dot{q} = \tau \quad (6)$$

$$J_h\ddot{q} = \tau_h - h(q - q_0) - d\dot{q} \quad (7)$$

where $r = \frac{J_m}{J_h}$. The structure of human joint model (7) can be used to represent both a passive and an active human condition. In the passive case the stiffness term $h(q - q_0)$ can be considered a linear and approximation of the gravitational torque and the damping term $d\dot{q}$ describes the mechanical joint friction due to muscle, tendons and articulations. In the active case the human is supposed to actively control the joint to reach a position q_0 and the damping and stiffness terms are mainly due to muscle contraction/co-contraction.

In both models (5) and (6) the dynamics of τ_h depends two parameters:

$$a = \frac{J_m}{k}, \quad c = (1 + \frac{J_m}{J_h}) = 1 + r. \quad (8)$$

Interestingly the inertia uncertainty is lumped in c while a can be known a-priori, as it characterizes the actuator. In a control application, the worst case is when c , or equivalently r , is high, showing high sensitivity to human joint model. This can be seen in (6) where r multiplies human forces/torques. Unfortunately this is often the case of SEAs where geared motors are usually adopted. In fact the (reflected) motor inertia J_m , which is proportional to r acts as a sensitivity gain. If one considers that the reflected motor inertia is augmented by a factor n^2 , where n is the transmission ratio, it follows that in most applications the system can be very sensitive to uncertainties

IV. SYSTEM CONTROL

In MRAC framework control specifications are given using a model reference. This is particularly convenient when it is easy to specify the desired bandwidth and damping/overshoot, as in a linear second order reference model. However in MRAC the reference model should have the same order of the plant to assure adaptation convergence (perfect tracking assumption). In this work we propose a slight modified approach to use a second order reference model even if the system (6-7) is a fourth order.

Lets start considering the following model reference

$$\ddot{\tau}_r(t) + \lambda_1\dot{\tau}_r(t) + \lambda_2\tau_r(t) = \lambda_2r(t) \quad (9)$$

where parameters λ_1 and λ_2 are chosen according to desired bandwidth and damping of the controlled system and $\tau_r(t)$ is the desired torque dynamics for τ_h in response to the bounded reference input $r(t)$.

If we consider the pure inertial model (5) we can achieve perfect tracking using the following control law

$$\tau_m = a(\ddot{\tau}_r - 2\lambda\dot{e} - \lambda^2e) + c\tau_h \quad (10)$$

where $e = \tau_h - \tau_r$ is the error between the system torque and the reference model torque, λ is a positive design parameter and a , c are defined in (8). If we compute the closed loop dynamics we obtain exponential convergence to the reference model with rate λ , that is

$$\dot{s} + \lambda s = 0 \quad (11)$$

where $s = \dot{e} + \lambda e$ is a measure of the tracking error whose convergence ($s \rightarrow 0$) imply the convergence of e and \dot{e} ($e \rightarrow 0$, $\dot{e} \rightarrow 0$), see section 7.1.1 in [19].

Inertia uncertainty can be taken into account by substituting the parameter c in (10) with its estimate \hat{c} , providing that

$$\dot{\hat{c}} = -\gamma s \tau_h \quad (12)$$

where γ is an adaptation gain to control the estimation speed. Stability of this adaptive controller can be proved within standard MRAC framework, as reported in appendix A. Unfortunately such stability analysis is not valid when considering a fourth order system (6-7) as discussed earlier. This invalidates the perfect tracking assumption and the stability analysis in appendix A. To overcome such problem we propose some candidate controllers that retain the simplicity of a second order reference model but that are stable when applied to the real fourth order system (6-7). Standard MRAC approach would lead to more complex control structures (to reach perfect tracking), fourth order model reference and high dimensional estimation. In fact such approach requires the estimate of eight variables because, differently from models (4) and (6), (known) actuator parameters results always in combination with (unknown) human joint parameters.

First we propose a controller based on five parameter estimate, then we show that the number of estimate can be reduced while increasing stability robustness.

A. An Adaptive Controller for SEAs

The first controller we propose is based on the compensation of certain dynamics aiming to make the τ/τ_h relation behaving like a second order system. We consider an arranged version of system (6)

$$a\ddot{\tau}_h + b\dot{\tau}_h + c\tau_h = \tau_m + h^*\theta - h_0 + d^*\dot{\theta} \quad (13)$$

where, naming $r = \frac{J_m}{J_h}$, we have the following parameters $a = \frac{J_m}{k}$, $b = r\frac{d}{k}$, $c = 1 + r(1 + \frac{h}{k})$, $h^* = rh$, $h_0 = h^*q_0$ and $d^* = rd$. Again the parameter a is known a priori while the others depend on human dynamics. The advantage of adopting this arrangement is that with respect to (6) it explicitly shows the full dynamics of the interaction torques (all the τ_h derivatives) and contains only collocated variables. In fact non-collocated feedback is known to have lower stability margins. In practical applications, where it is quite usual to have unmodeled dynamics, combining adaptivity with low gain margins can actually presents a risk of instability.

In the light of this consideration we propose the following adaptive controller

$$\tau_m = a(\ddot{\tau}_r - 2\lambda\dot{e} - \lambda^2 e) + \hat{b}\dot{\tau}_h + \hat{c}\tau_h \quad (14)$$

$$\begin{aligned} -\hat{h}\theta - \hat{d}\dot{\theta} + \hat{h}_0 - \delta \\ \dot{\hat{b}} = -\rho s \dot{\tau}_h \quad \dot{\hat{c}} = -\rho s \tau_h \quad \dot{\hat{d}} = -\rho s \dot{\theta} \\ \dot{\hat{h}} = -\rho s \theta \quad \dot{\hat{h}}_0 = -\rho s \end{aligned} \quad (15)$$

where $s = \dot{e} + \lambda e$, $e = \tau_h - \tau_r$ is the error with respect to the reference model (9) and ρ is an adaptation gain. In the following theorem we prove that this control law can stabilize the fourth order system (6-7) by using a second order reference model. This result will be used also in the rest of the paper and, in our opinion, it is an original contribution. To achieve the proof we introduce in the control law the term

$$\delta = \epsilon \frac{e}{s} \dot{q} \quad (16)$$

where ϵ is an arbitrarily small positive parameter. Note that λ is usually chosen as high as possible thus in practice $\delta \simeq \frac{\epsilon}{\lambda} \dot{q}$ approximates the form of a damper.

Theorem 1. *Given the system the system (6-7) where τ is determined by the adaptive control law (14) with adaptation (15) and assuming a steady state reference model condition $\tau_r(t) = \bar{\tau}_r$, then the trajectories of states e , \dot{e} , \dot{q} are asymptotically stable (AS) and estimation errors and q are marginally stable.*

Proof: Consider the following Lyapunov function $V(t) = V_s(t) + V_q(t) + V_p(t)$ where

$$V_s(t) = \frac{1}{2} a s^2, \quad V_q(t) = \frac{1}{2} f \tilde{q}^2 + \frac{1}{2} g \dot{\tilde{q}}^2 \quad (17)$$

with $\tilde{q} = q - \bar{q}$, $\bar{q} = \frac{\bar{\tau}_r}{J_h} + q_0$ and

$$V_p(t) = \frac{1}{2\rho} (\tilde{b}^2 + \tilde{c}^2 + \tilde{d}^2 + \tilde{h}^2) \quad (18)$$

where, naming p a generic parameter, \tilde{p} represents the parameter estimation error $\tilde{p} = \hat{p} - p$. For better understandability we first prove the stability assuming perfect estimation. In such case the closed loop dynamics is $a(\dot{s} + \lambda s) = -\delta$ and the Lyapunov time derivative is

$$\dot{V}_s = a s \dot{s} = -a \lambda s^2 - s \delta. \quad (19)$$

For the states q and \dot{q} we have $\dot{V}_q = f q \dot{q} - f \bar{q} \dot{q} + g \dot{\tilde{q}} \ddot{\tilde{q}}$ and from (7) we have $\dot{q} \ddot{q} = \frac{1}{J_h} [\tau_h \dot{q} - h(q \dot{q} - q_0 \dot{q}) - d \dot{q}^2]$ and, by choosing $f = h\epsilon$ and $g = J_h\epsilon$, we find

$$\dot{V}_q = \epsilon(\tau_h \dot{q} + h q_0 \dot{q} - h \bar{q} \dot{q} - d \dot{q}^2).$$

Now substituting δ as in (16) and considering that $\tau_h = e + \bar{\tau}_r$ we can obtain $\dot{V} = -a \lambda s^2 + \epsilon \dot{q}(\bar{\tau}_r + h q_0 - h \bar{q}) - \epsilon d \dot{q}^2$. Finally we eliminate the second term by substituting the expression of \bar{q} , leading to

$$\dot{V} = -a \lambda s^2 - \epsilon d \dot{q}^2 \leq 0. \quad (20)$$

If now we introduce the parameter dynamics, the estimation errors appears in

$$\dot{V}_s = -a \lambda s^2 + s(\tilde{b} \dot{\tau}_h + \tilde{c} \tau_h + \tilde{d} \dot{\theta} + \tilde{h} \theta + \tilde{h}_0) - s \delta. \quad (21)$$

Summing $\dot{V}_p = \frac{1}{2\rho}(\tilde{b}\dot{\tau}_h + \tilde{c}\dot{\tau}_h + \tilde{d}\dot{\theta} + \tilde{h}\dot{\theta})$ and substituting the proposed adaptation (15) one obtain $\dot{V}_{s+p} = -a \lambda s^2 - s \delta$ that is equal to (19). Then the demonstration proceed as in the previous case leading to (20) that imply global marginal stability for state trajectories. Finally using Barbalat's lemma it can be proved that states s , \dot{q} are asymptotic stable. ■

B. A Simpler and More Robust Adaptive controller

The control strategy proposed in the previous section is theoretically sound and we will show in section V that under certain conditions it works with very high performance. However it is known that such a multi-dimensional estimation can be a hazard in practice, especially when there is a mismatch between the model structure and the human dynamics and/or we do not have persistent excitation. We show that using fewer parameters it is possible to have performance similar to algorithm (14) with increased robustness, i.e. we can consider a more generic human joint model

$$J_h \ddot{q} + Z_h(q, \dot{q}, q_0) = \tau_h \quad (22)$$

where Z_h represents non linear stiffness and damping forces. With respect to (7) this is a more realistic description because human muscle are strongly non linear. As muscle forces are also limited we introduce the following bound

$$|Z_h(q, \dot{q}, q_0)| \leq \Omega \quad (23)$$

with $\Omega \geq 0$. By using this joint model the interaction dynamics can be arranged as

$$a \ddot{\tau}_h + c \tau_h = \tau + r Z_h(q, \dot{q}, q_0) \quad (24)$$

with parameters a and c as defined in (8) and $r = \frac{J_m}{J_h}$. Note that joint model (22) can represent also gravitational and apparent forces.

We propose the following control law

$$\tau_m = a(\ddot{\tau}_r - 2\lambda\dot{e} - \lambda^2 e) + \hat{c}\tau_h \quad (25)$$

with adaptation

$$\dot{\hat{c}} = -\rho(s\tau_h + \sigma\hat{c}) \quad (26)$$

where $e = \tau_h - \tau_r$ is the error with respect to the reference model (9) and $s = \dot{e} + \lambda e$. The parameter ρ is an adaptation gain and σ is a forgetting factor that was introduced in [14].

Theorem 2. *Given the system (24), with the assumption of bounded human forces (23), and the adaptive control law (25-26), then state trajectories $s(t)$ and $\tilde{c}(t)$ are globally uniformly ultimately bounded (UUB).*

Proof: Consider the system (24) where we have again a known a priori. Consider the Lyapunov function $V(t) = V_s(t) + V_p(t)$ with V_s as before in (17) and $V_p = \frac{1}{2\rho} \tilde{c}^2$. By applying the control law (25) with adaptation (26) to system (24), (23) we find

$$\begin{aligned} \dot{V}_s &= a s \dot{s} = -a \lambda s^2 + s r Z_h + s \tilde{c} \tau_h \\ \dot{V}_p &= \frac{1}{\rho} \tilde{c} \dot{\tilde{c}} = -s \tilde{c} \tau_h - \sigma \tilde{c}^2 - \sigma c \tilde{c}. \end{aligned} \quad (27)$$

where $\tilde{c} = \hat{c} - c$. By summing \dot{V}_s and \dot{V}_p we have

$$\dot{V} = -a \lambda s^2 + r Z_h s - \sigma \tilde{c}^2 - \sigma c \tilde{c}. \quad (28)$$

Then if we analyze the Lyapunov derivative outside the region

$$-a\lambda s^2 + srZ_h - \sigma\tilde{c}^2 - \sigma c\tilde{c} = 0 \quad (29)$$

we have $\dot{V} < 0$. Thus outside (29) the trajectory behaves as if the origin was uniformly asymptotically stable. Consequently, the function V will continue decreasing until the trajectory enters the region (29) in finite time and remains in. Formally by choosing β such that $|\beta| > r\Omega$ we have that $\dot{V} < 0$ is satisfied on every boundary expressed as

$$a\lambda s^2 - s\beta + \sigma\tilde{c}^2 - \sigma c\tilde{c} = 0, \quad (30)$$

meaning that trajectories $s(t)$ and $\tilde{c}(t)$ are globally uniformly bounded. Moreover an ultimate bound can be computed by substituting $\beta = r\Omega$ in (30). ■

It is easy to show that the boundary area decreases monotonically with λ and that boundedness of s imply boundedness of $e(t)$ and $\dot{e}(t)$, see section 7.1.1 in [19] for a proof. We conclude that by a proper choice of λ the attracting region can be sufficiently small and we can have acceptable tracking errors. Figure 2 graphically represents the attracting region of theorem in the state plane (left) and in the error phase plane (right).

Theorem 2 is again, in our opinion, original. In fact, w.r.t standard MRAC, control law (25) embeds only a partial system model, as it discards the dynamics of q and \dot{q} .

An interesting observation is that a high human joint inertia helps to improve accuracy (this is because β decreases with J_h). In fact the control task is usually facilitated in case of high coupled impedance. Here we explain this effect for model (6-7). If we consider the limit cases of infinite damping or stiffness ($h \rightarrow \infty$ or $d \rightarrow \infty$) the human joint position q becomes infinitely stiff thus imperturbable. This make the system model (6-7) become

$$a\ddot{\tau}_h = \tau_m - \tau_h. \quad (31)$$

Then by applying the control law (25) with adaptation (26) we are in the case of appendix A with the parameter c equal to 1. In this case the controlled system is asymptotically stable, i.e. it has infinite accuracy. This also shows that it is a good choice to adapt the parameter c . When the environment change dynamics from (6-7) to (31) the parameter change its meaning and the controller approaches better accuracy.

Finally we propose a similar adaptive algorithm that uses the additional parameter \hat{b} to estimate the human damping or dissipation. The proposed control law is

$$\tau_m = a(\ddot{\tau}_r - 2\lambda\dot{e} - \lambda^2 e) + \hat{b}\dot{\tau}_h + \hat{c}\tau_h - \delta \quad (32)$$

with adaptation dynamics given by

$$\dot{\hat{b}} = -\rho(s\dot{\tau}_h + \sigma\hat{b}), \quad \dot{\hat{c}} = -\rho(s\tau_h + \sigma\hat{c}). \quad (33)$$

This control law is expected to perform better because it can distinguish between the stiffness and the damping (dissipative) part of human dynamics. Stability of this controller can be analyzed in a similar way to the previous case but considering the linear human join model (7) which separates stiffness and damping forces. In this case we can also prove boundedness of human displacement \tilde{q} and velocity $\dot{\tilde{q}}$.

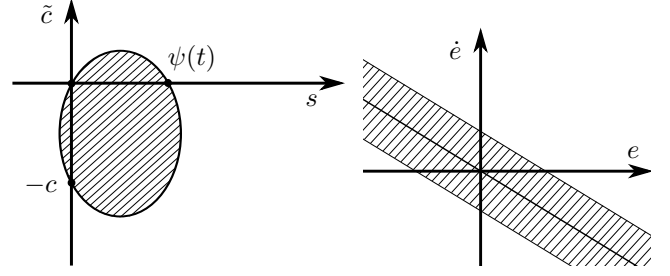


Figure 2. On the left we draw a representation of the attracting region (29) where $\psi(t) = rZ_h$. When Z_h is negative the region is mirrored on negative x-axis. On the right we represent only the states e , \dot{e} and one can see the region mapped on the error phase plane.

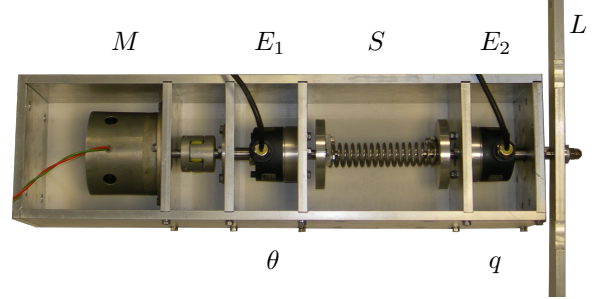


Figure 3. The SEA prototype used as testbed. The motor M is connected to the torsional spring S and the angular quantities θ and q are measured by encoders E_1 and E_2 respectively. L is the arm support that is a pure inertial load when the system is not interacting with a human joint.

Theorem 3. *Given the system (6-7), constrained to $|h(\theta - q_0) + r\dot{\theta}| \leq \Omega$, and the adaptive control law (25-26), assuming a steady state reference model condition $\tau_r(t) = \bar{\tau}_r$, then state trajectories $s(t)$, \dot{q} , \tilde{q} , $\tilde{c}(t)$ and $\tilde{b}(t)$ are globally uniformly ultimately bounded.*

To be noted that Theorem 3 uses both the original findings of Theorems 1 and 2. Control law (25-26) stabilizes the human displacement \tilde{q} and discards the dynamics of q and \dot{q} .

V. EXPERIMENTAL RESULTS

The experimental setup is the SEA prototype shown in figure 3, composed of a DC torque motor connected in series to a spring and then to a metal bar simulating the support for a human limb. Two high precision encoders are used to measure motor position and spring displacement. Velocities are obtained by measuring pulse inter-periods, using hardware interrupts.

The control system runs on a standard PC equipped with a quad-core processor and a real-time Linux kernel. Real-time is obtained using a process with kernel-like priority and system sleep function with nano second granularity. The control process runs at $3KHz$ and communicates with the motor drive and the sensor electronics via Ethercat protocol at the same rate.

System parameters have been estimated using a procedure similar to the one described in [4] and are reported in Table I. In the experiments the metal support in figure 3 have been replaced by a wood frame to create a worst-case working

Parameter	Symbol	Mean Value
Spring Stiffness	k	1.040 Nm/rad
Torque constant	k_t	0.42 Nm/A
Motor inertia	J_m	0.00041 Kg/m ²
Wood Load Inertia	J_W	0.00025 Kg/m ²
Metal Load Inertia	J_M	0.00390 Kg/m ²
a	J_m/k	0.00039
c - Wood Load	$1 + J_m/J_W$	2.62
c - Metal Load	$1 + J_m/J_M$	1.10

Table I
SYSTEM PARAMETERS

Joint	Human inertia J_h	Motor Inertia $n^2 J_m$	n
hip (swing)	$\sim 0.5 \div 5 \text{ Kg} \cdot \text{m}^2$	$\sim 0.8 \div 8 \text{ Kg} \cdot \text{m}^2$	$\sim 200 \div 800$
knee (swing)	$\sim 0.4 \text{ Kg} \cdot \text{m}^2$	$\sim 0.6 \text{ Kg} \cdot \text{m}^2$	$\sim 50 \div 250$
elbow	$\sim 0.08 \text{ Kg} \cdot \text{m}^2$	$\sim 0.1 \text{ Kg} \cdot \text{m}^2$	$\sim 30 \div 100$
wrist	$\sim 0.0015 \text{ Kg} \cdot \text{m}^2$	$\sim 0.002 \text{ Kg} \cdot \text{m}^2$	$\sim 15 \div 40$

Table II
MOTOR CHOICES WHERE $c \sim 2.5$

condition. This is because we use a direct drive transmission and we need to have a small load inertia (less or comparable with J_m) to get pessimistic values for the parameter c , as defined in (8). With the wood load we achieve $c = 2.62$. To understand if our setup is representative of a real rehabilitation scenario we report in Table II some pairs (human inertia, motor inertia) that are characterized by $c \sim 2.5$ (or equivalently $r \sim 1.5$) which defines the sensitivity to environment dynamics. Approximate values for human inertia are derived from bio-mechanical measurements in [8], [28]. We report also examples of transmission ratios n that are computed considering a motor shaft of $10^{-6} \div 10^{-5} \text{ Kg} \cdot \text{m}^2$. Reported values seem to the author as seen in practical applications.

The objective of experiments is to test the controllers in a worst case scenario when the system dramatically changes its dynamics. To this aim we designed the following experiments. At the beginning we create a high impedance condition by holding the wood frame by hand and trying to be as stiff as possible ($c \sim 1$). Then after some seconds we release the frame to create a low impedance condition ($c \sim 2.5$). The sequence can be repeated to test the stability at the impact, when we hit the load to hold it for the second time. In this case we call the experiment “intermittent interaction test”. Note that, as the wood load inertia is very low, the impact velocity can be very high.

To have a baseline we show first the behavior of PB controllers. The passive PID controller (3) is tuned with $P = 10$ and $D = 0.1$ and $I = 4$ with a 1Hz roll-off frequency (accordingly to passivity constraints). The torque reference is low-pass filtered with a cut off frequency of 35Hz , to avoid too oscillatory responses in case of discontinuities and to make a fair comparison with MRAC as we will use also a 35Hz reference model. Results of sinusoidal torque tracking

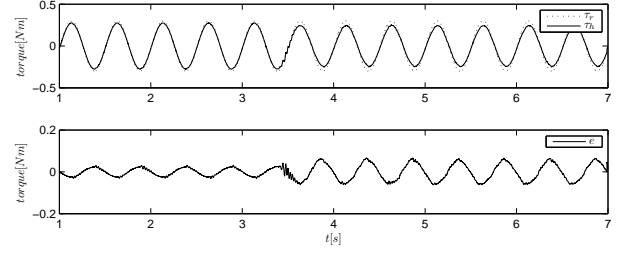


Figure 4. Response of algorithm (3) using a sinusoidal reference τ_r . The load is firstly hold by hand and then released at about $t = 3.5\text{s}$.

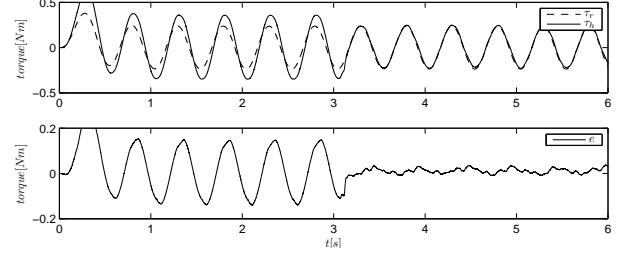


Figure 5. Response of a PD controller tuned on free wood load condition.

are shown in figure 4. Errors result quite low in the high impedance case but when the load is released errors increase and evident oscillations occur. To have a high performance in the low impedance condition we avoid the integral term and use a fix-gain version of algorithm (25) considering $c = 2.62$. This algorithm is passive because by setting $\lambda = 120$ we have $P = a\lambda^2 - 2.62 > 0$ and $D = 2a\lambda > 0$. Figure 5 shows that while the response is accurate in the low impedance case, we have significant overshoots when the impedance is high.

The outcomes of proposed adaptive algorithms are shown in figure 6-9. In all the following tests we used a critically damped 35Hz reference model and a convergence rate $\lambda = 120$. Larger values for λ lead to noise amplification. Estimated parameters are initialized to zero. The plotted error e is computed with respect to the reference model thus it

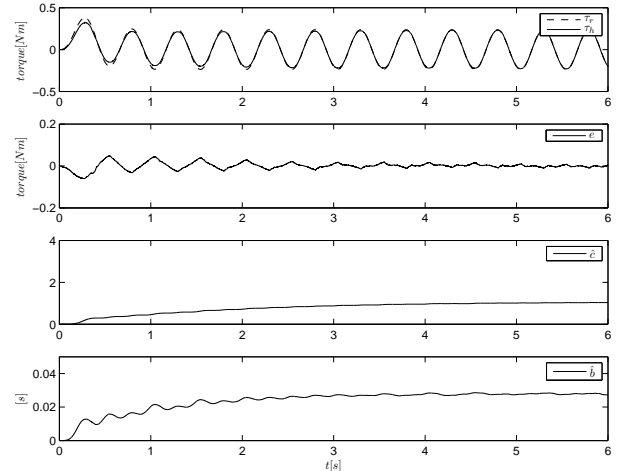


Figure 6. Performance of control law (14) in response to a sinusoidal reference during the “hold by hand” test.

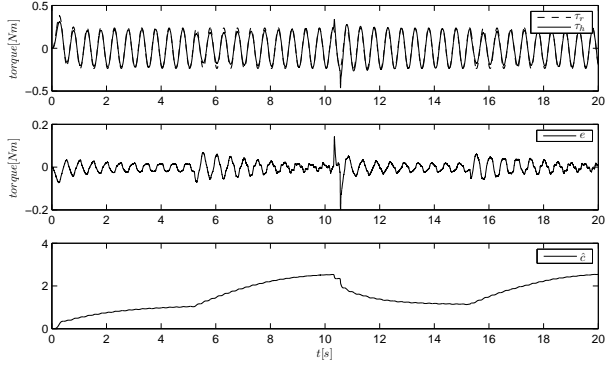


Figure 7. The control law (25) in response to a sinusoidal reference in the “intermittent interaction test”. The error peak occurs when we hit the load to hold it again.

is not only a measure of accuracy but also of specification fulfillment. Figure 6 shows the behavior of algorithm (14) when only the high impedance is applied. It is possible to see a final very small error as well as convergence of parameters \hat{b} and \hat{c} . Adaptation transient is kept slow on purpose to put in evidence the effects of parameter learning. In a real-life application convergence can take less than one second without generating oscillations, as we will show in the following. We do not expect that parameters converge to their true value because estimation errors are proved to be marginally stable. In fact, in the experiment of figure 6, parameters \hat{d} and \hat{h}_o (not showed) remain low, especially in the case of \hat{d} and \hat{h} that remain very close to zero. Unfortunately in the low impedance case, when the load is unconstrained, this algorithm has worse behavior and we observed instability. This is probably due to the fact that in the low impedance case the load is let be free and as a consequence the environment does not display any stiffness. This absence of the stiffness information can cause a misbehavior of the estimation procedure which searches for a modeled stiffness which is actually missing in the real world. This causes that both \hat{h} and \hat{h}_o estimates are prone to divergence. Even from a system identification point of view, when the environment does not display a stiffness/damping component, our model results over-parametrized, leading to the risk of a non consistent estimation.

On the other hand, the simplified algorithm (25) shows a very stable behavior. We made a stress test by cyclically holding the load by hand and releasing it, thus testing also the impact stability. Figure 7 shows data from this “intermittent interaction test”. Here in particular the load is first held by hand and released after about 5s. Then, at time $t = 10$ the moving load is held again (a hit occurs) and then released after 5s. Figure 7 shows that when the interaction changes the parameter adapts showing noticeable decreasing error transients. Also we have the evidence of a non-biased estimation. When the load is free \hat{c} converges to the correct value in Table I otherwise when the load is held by hand $c \sim 1$.

The controller (32) shows the best outcome, as shown in figures 8 and 9. It combines the high tracking performances of algorithm (14) with the high robustness of its simplified version (25). In fact when the joint is held by the human it

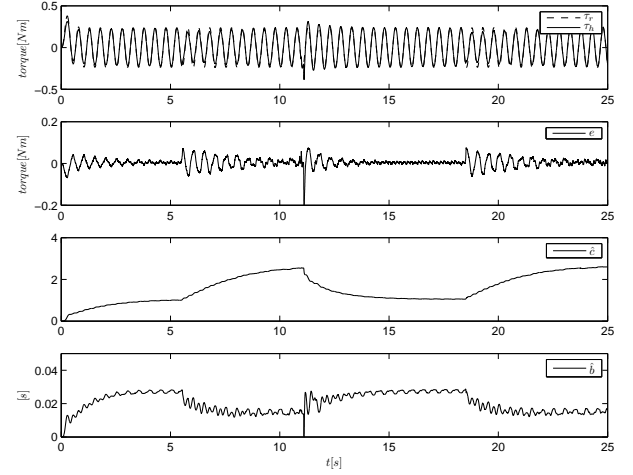


Figure 8. The control law (32) in response to a sinusoidal reference in the “intermittent interaction test”. The error peak occurs when we hit the load to hold it again.

	Low Impedance				High Impedance			
	Passive		Adaptive		Passive		Adaptive	
	PID	PD	\hat{c}	\hat{b}, \hat{c}	PID	PD	\hat{c}	\hat{b}, \hat{c}
RMS	69.0	15.1	9.3	5.8	27.3	102.6	13.9	6.2
σ_{RMS}	0.47	1.5	0.99	0.30	0.28	1.0	1.2	0.54
Max	99.6	26.3	17.2	12.1	41.4	146.5	18.9	13.9
σ_{Max}	0.84	2.9	2.6	1.1	0.67	1.1	3.6	1.3

Table III
COMPARISON OF RMS AND MAXIMUM ERROR [$10^{-3}Nm$]

is subject to some energy dissipation that leads the controller to change its derivative gain and achieve performances similar to that of figure 6. W.r.t figure 7 this controller shows improved accuracy and similar robust behavior when the external impedance changes. These results are shown in figure 8 where one can notice the non biased estimation of c .

In figure 9 we show that the adaptation dynamics can be tuned to be very fast without degrading the maximum reachable precision nor the stability. If we compare this plot with PB control responses reported in figures 4 and 5 it is immediate to notice the improvements. A quantitative comparison of the described controllers is reported in Table III. Here each controller is tested in the high and low impedance condition separately. Root mean square (RMS) and maximum errors are reported for each case. Due to the uncertain nature of pHRI these indexes are computed for each reference period² and considered as random processes. Relative means and standard deviations are reported in Table III. Performance results greatly improved by adaptive controller. Considering 3σ intervals there are no statistically significant differences between performances in the high and in low impedance conditions, especially in the case of control law (32).

²We have a total of 240 periods for each controller, 120 in the high impedance condition and 120 in the low.

1.Control Law 2.System Model 3.Adaptation	Theoretical Stability	Experimental Outcome
1.Eq.(14) 2.Eq.(6-7) 3.Param. b, c, d, h, h_0	AS. only when coupled with 2 nd order linear impedance	High Performance, Poor Stability (absence of environmental stiffness leads to instability)
1.Eq.(25) 2.Eq.(23-24) 3.Param. c	Globally UUB when coupled with the generic impedance (24-23). AS when coupled with “infinite” impedance (infinite inertia or stiffness or damping etc.)	Medium Performance, Robust stability (it never goes to instability despite stress tests)
1.Eq.(32) 2.Eq.(6-7) 3.Param. b, c	Similar to the previous case. Here the boundedness proof includes also states \tilde{q} and \dot{q} .	High Performances, Robust Stability

Table IV
SUMMARY OF PAPER RESULTS

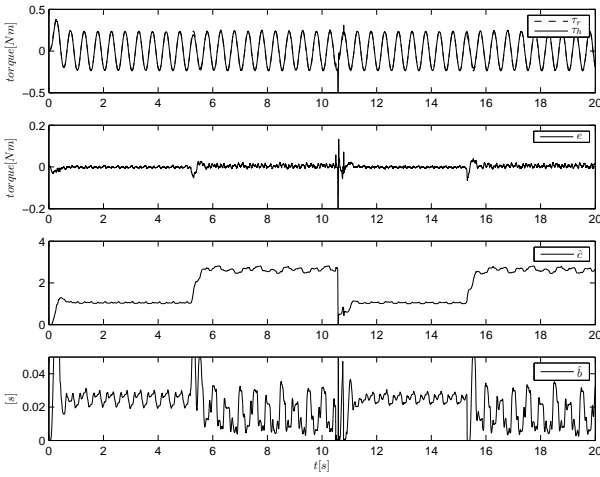


Figure 9. The control law (32) with high adaptation gains in response to a sinusoidal reference in the “intermittent interaction test”.

VI. CONCLUSIONS

We proposed two simple and effective force control algorithms for SEAs (equations (25) and (32)) that enable stable and predictable interaction with a human both in passive and active configuration. With respect to existing PB controllers, the proposed solutions have several advantages. First they can meet desired force control specifications even when the coupled dynamics changes, second they do not need a tuning process as they are patient-specific and joint-specific self-tuning controllers, third they proved to be very accurate. We think that these advantages are of paramount importance for control engineers to build rehabilitation or assistive devices. We demonstrated the quality of proposed controllers by discussing their theoretical properties and providing experimental validation. A brief view of achievement is summarized in Table IV where for each controller we report related human joint model and adaptation parameters.

For future work we plan two objectives. The first is to investigate a passive versions of the proposed adaptive approach. The second is to introduce adaptation mechanisms that are not only based on tracking errors but also on prediction errors.

APPENDIX

A. Stability analysis of control law (10) on model (5)

The following candidate Lyapunov function for the controlled system comprehending the plant (5), the control law (10) and the adaptation law (12) is chosen

$$V = \frac{1}{2}[as^2 + \frac{1}{\gamma}\tilde{c}^2] \geq 0$$

where $s = \dot{e} + \lambda e$ is a measure of the tracking error and $\tilde{c} = \hat{c} - c$ is the parameter estimation error. By computing the time derivative one can find

$$\dot{V} = as\dot{s} + \frac{1}{\gamma}\tilde{c}\dot{\tilde{c}} \quad (34)$$

where computation of \dot{s} needs the knowledge of the closed loop dynamics. This can be obtained by substituting equation (10) into (5) leading to $\dot{s} = \frac{\tilde{c}\tau_h}{a} - \lambda s$ and then to

$$\dot{V} = -a\lambda s^2 + \tilde{c}s\tau_h + \frac{1}{\gamma}\tilde{c}\dot{\tilde{c}}. \quad (35)$$

By applying the adaptation law $\dot{\tilde{c}} = \dot{\hat{c}} - \dot{c} = -\gamma s\tau_h$ in (35) we finally have $\dot{V} = -a\lambda s^2 \leq 0$ that imply global marginal stability for the system, thus bounded s and \tilde{c} . To prove convergence to zero of s we can use Barbalat’s lemma. Given a lower bounded V it requires $\dot{V} \leq 0$ and \dot{V} to be uniformly continuous in time then it proves that $s \rightarrow 0$ for $t \rightarrow \infty$. A sufficient condition for uniform continuity is a bounded second order derivative, that can be computed as

$$\ddot{V} = -2\lambda\tilde{c}s\tau_h + 2a(\lambda s)^2. \quad (36)$$

Then asymptotic stability of s can be proved considering that we already proved the boundedness of s , e and \tilde{c} and the human force $\tau_h = \tau_r + e$ is limited if we apply bounded desired force $r(t)$ to the stable reference model (9).

REFERENCES

- [1] SP Buerger and Neville Hogan. Complementary stability and loop shaping for improved human-robot interaction. *Robotics, IEEE Transactions on*, 23(2):232–244, 2007.
- [2] Stephen Buerger and Neville Hogan. Relaxing Passivity for Human-Robot Interaction. *2006 IEEE/RSJ International Conference on Intelligent Robots and Systems*, pages 4570–4575, October 2006.

- [3] Lance L Cai, Andy J Fong, Chad K Otsoshi, Yongqiang Liang, Joel W Burdick, Roland R Roy, and V Reggie Edgerton. Implications of assist-as-needed robotic step training after a complete spinal cord injury on intrinsic strategies of motor learning. *The Journal of neuroscience : the official journal of the Society for Neuroscience*, 26(41):10564–8, October 2006.
- [4] Andrea Calanca, L.M. Capisani, Antonella Ferrara, and Lorenza Magnani. MIMO closed loop identification of an industrial robot. *IEEE Transactions on Control Systems Technology*, 19(5):1214–1224, 2011.
- [5] Andrea Calanca, S Piazza, and Paolo Fiorini. Force Control System for Pneumatic Actuators of an Active Gait Orthosis. In *Biomedical Robotics and Biomechatronics (BioRob), 2010 3rd IEEE RAS and EMBS International Conference on. 26-29 Sep, 849-854, 2010*, pages 64–69, Tokyo, 2010.
- [6] Andrea Calanca, S Piazza, and Paolo Fiorini. A motor learning oriented, compliant and mobile Gait Orthosis. *Applied Bionics and Biomechanics*, 9(1):15–27, 2012.
- [7] Alexander Duschau-Wicke, Joachim von Zitzewitz, Andrea Caprez, Lars Lunenburger, and Robert Riener. Path control: a method for patient-cooperative robot-aided gait rehabilitation. *IEEE transactions on neural systems and rehabilitation engineering : a publication of the IEEE Engineering in Medicine and Biology Society*, 18(1):38–48, February 2010.
- [8] WS Erdmann. Geometry and inertia of the human body-review of research. *Acta of Bioengineering and Biomechanics*, 1(1):23–35, 1999.
- [9] M. Ferraro, J. J. Palazzolo, J. Krol, H. I. Krebs, N. Hogan, and B. T. Volpe. Robotaided sensorimotor arm training improves outcome in patients with chronic stroke. *Neurology*, 61(11):1604–7, 2003.
- [10] R E Kearney, R B Stein, and L Parameswaran. Identification of intrinsic and reflex contributions to human ankle stiffness dynamics. *IEEE transactions on bio-medical engineering*, 44(6):493–504, June 1997.
- [11] Kyoungchul Kong, Student Member, and Joonbum Bae. Control of Rotary Series Elastic Actuator for Ideal Force-Mode Actuation in Human-Robot Interaction Applications. *IEEE/ASME International Conference on Mechatronics*, 14(1):105–118, 2009.
- [12] H I Krebs, L Dipietro, B T Volpe, and N Hogan. Rehabilitation Robotics : Performance-Based Progressive Robot-Assisted Therapy. *Autonomous Robots*, 15:7–20, 2003.
- [13] Kong Kyoungchul, Moon Hyosang, Jeon Doyoung, and Tomizuka Masayoshi. Control of an Exoskeleton for Realization of Aquatic Therapy Effects. *IEEE/ASME Transactions on Mechatronics*, 15:191–200, 2010.
- [14] Kumpati S Narendra and Anuradha M Annaswamy. Robust Adaptive Control. *1984 American Control Conference*, (TFRT-1035):848, 1985.
- [15] Jerome J Palazzolo. *Robotic Technology to Aid and Assess recovery and learning in stroke patients*. PhD thesis, Massachusetts Institute of Technology., 2005.
- [16] Gill A Pratt and M.M. Williamson. Series Elastic Actuators. In *International Conference on Intelligent Robots and Systems*, volume 1, pages 399–406. IEEE, 1995.
- [17] Gill A Pratt, Pace Willisson, and Clive Bolton. Late motor processing in low-impedance robots: Impedance control of series-elastic actuators. In *American Control Conference*, pages 3245–3251, 2004.
- [18] Jerry Pratt, Chee-meng Chew, Ann Torres, Peter Dilworth, and Gill Pratt. Virtual model control: An intuitive approach for bipedal locomotion. *International Journal of Robotics Research*, 20(2):129–143, 2001.
- [19] Jean-Jacques E Slotine and Weiping Li. *Applied Nonlinear Control*, volume 62. Prentice Hall, 1991.
- [20] R B Stein, E P Zehr, M K Lebiadowska, D B Popović, a Scheiner, and H J Chizeck. Estimating mechanical parameters of leg segments in individuals with and without physical disabilities. *IEEE transactions on rehabilitation engineering : a publication of the IEEE Engineering in Medicine and Biology Society*, 4(3):201–11, September 1996.
- [21] S Stroeve. Impedance characteristics of a neuromusculoskeletal model of the human arm I. Posture control. *Biological cybernetics*, 81(5-6):475–94, November 1999.
- [22] K P Tee, E Burdet, C M Chew, and T E Milner. A model of force and impedance in human arm movements. *Biological cybernetics*, 90(5):368–75, May 2004.
- [23] Heike Vallery. *Stable and User-Controlled Assistance of Human Motor Function*. PhD thesis, University of Munchen, 2009.
- [24] Heike Vallery, Ralf Ekkelenkamp, Herman van der Kooij, and Martin Buss. Passive and accurate torque control of series elastic actuators. *2007 IEEE/RSJ International Conference on Intelligent Robots and Systems*, pages 3534–3538, October 2007.
- [25] Heike Vallery, Edwin H F van Asseldonk, Martin Buss, and Herman van der Kooij. Reference trajectory generation for rehabilitation robots: complementary limb motion estimation. *IEEE transactions on neural systems and rehabilitation engineering : a publication of the IEEE Engineering in Medicine and Biology Society*, 17(1):23–30, February 2009.
- [26] Heike Vallery, Jan Veneman, Edwin H F van Asseldonk, Ralf Ekkelenkamp, Martin Buss, and Herman van Der Kooij. Compliant actuation of rehabilitation robots. *IEEE Robotics & Automation Magazine*, 15(3):60–69, September 2008.
- [27] Y Xu and J M Hollerbach. A robust ensemble data method for identification of human joint mechanical properties during movement. *IEEE transactions on bio-medical engineering*, 46(4):409–19, April 1999.
- [28] Vladimir M. Zatsiorsky. *Kinetics of Human Motion*. 2002.